Volume 15 | Number 8 | August 2016 | Pages 951–1082

Photochemical & Photobiological Sciences

An international journal

www.rsc.org/pps

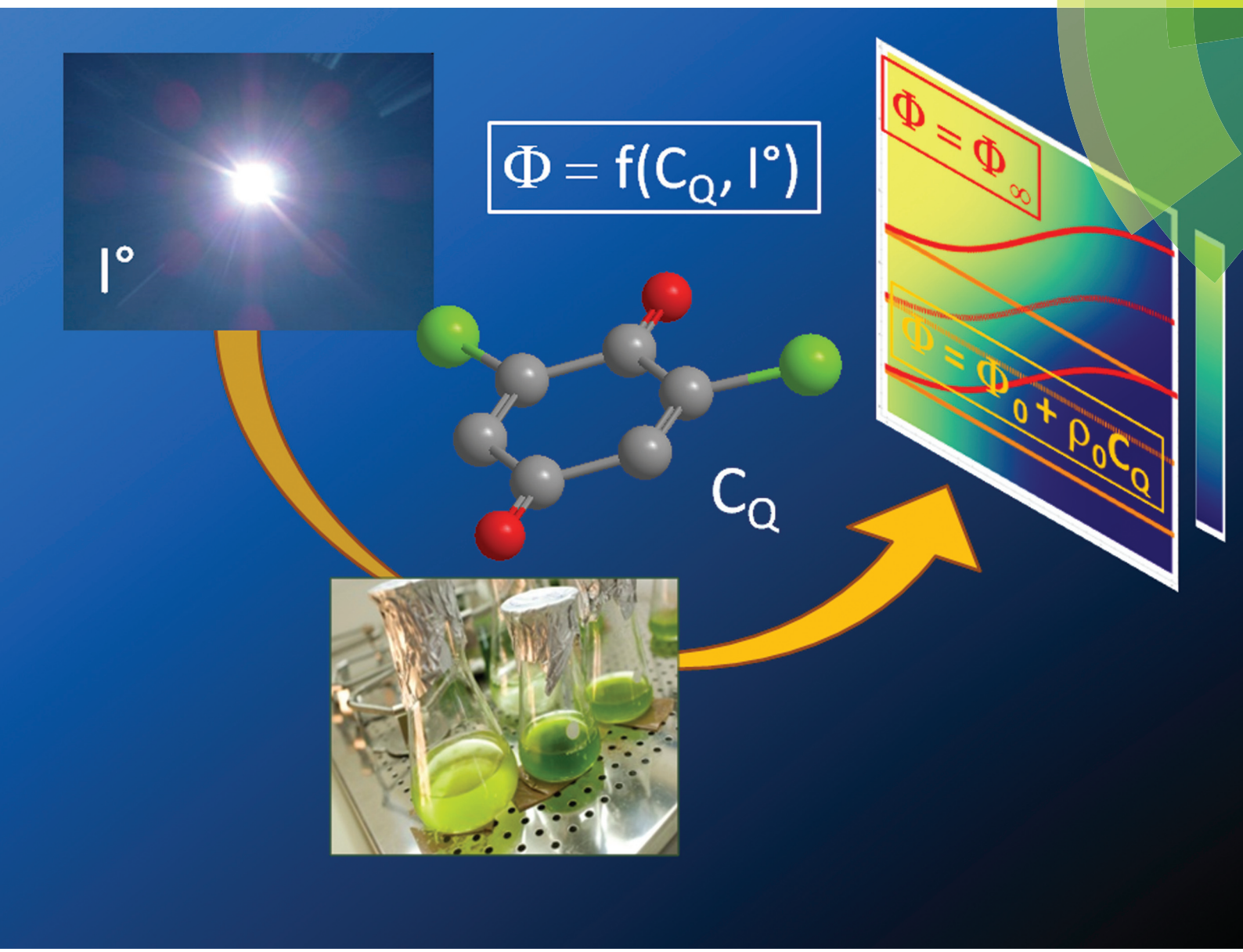

ISSN 1474-905X

ROYAL SOCIETY OF CHEMISTRY

EPA ESP KOREAN SOCIETY OF PHOTOSCIENCE AOSP

Photochemical & Photobiological Sciences

PAPER

View Article Online
View Journal | View Issue

Cite this: *Photochem. Photobiol. Sci.*, 2016, **15**, 969

Mechanism and analyses for extracting photosynthetic electrons using exogenous quinones – what makes a good extraction pathway?†

G. Longatte,‡[a,b] F. Rappaport,§[c] F.-A. Wollman,[c] M. Guille-Collignon[a,b] and F. Lemaître*[a,b]

Plants or algae take many benefits from oxygenic photosynthesis by converting solar energy into chemical energy through the synthesis of carbohydrates from carbon dioxide and water. However, the overall yield of this process is rather low (about 4% of the total energy available from sunlight is converted into chemical energy). This is the principal reason why recently many studies have been devoted to extraction of photosynthetic electrons in order to produce a sustainable electric current. Practically, the electron transfer occurs between the photosynthetic organism and an electrode and can be assisted by an exogenous mediator, mainly a quinone. In this regard, we recently reported on a method involving fluorescence measurements to estimate the ability of different quinones to extract photosynthetic electrons from a mutant of *Chlamydomonas reinhardtii*. In the present work, we used the same kind of methodology to establish a zone diagram for predicting the most suitable experimental conditions to extract photoelectrons from intact algae (quinone concentration and light intensity) as a function of the purpose of the study. This will provide further insights into the extraction mechanism of photosynthetic electrons using exogenous quinones. Indeed fluorescence measurements allowed us to model the capacity of photosynthetic algae to donate electrons to an exogenous quinone by considering a numerical parameter called "open center ratio" which is related to the Photosystem II acceptor redox state. Then, using it as a proxy for investigating the extraction of photosynthetic electrons by means of an exogenous quinone, 2,6-DCBQ, we suggested an extraction mechanism that was globally found consistent with the experimentally extracted parameters.

Received 17th March 2016,
Accepted 23rd June 2016

DOI: 10.1039/c6pp00076b

www.rsc.org/pps

Introduction

Extraction of photosynthetic electrons to produce an amenable electric current is a recent and important research topic. Indeed photosynthesis (Fig. 1) has overall a low yield *in vivo* (a few % of the total energy available from sunlight is converted into chemical energy). Among its various limitations, such a low yield is related to the saturation of the photochemical conversion (rate limiting electron transfer steps occurring downstream of Photosystem II) but not to the quantum efficiencies of photosystems (close to 100% under optimal conditions).[1] That is why photosynthesis is viewed as a promising and unexploited reservoir to produce electricity by harvesting electrons among the photosynthetic chain. Furthermore, under high light conditions, the saturation of the photochemical conversion can lead to photoinhibition, *i.e.* formation of reactive species which can induce some biological damage while overwhelming the usual photorepair pathways.[2] Therefore, extracting photosynthetic electrons is expected to alleviate the saturation and thus to limit photoinhibition.

Several strategies for harvesting photosynthetic electrons have been implemented in recent years. Although all of them clearly involve an electrode for collecting electrons from the photosynthetic organism, the nature of the biological target and the experimental conditions used are rather different.

[a]*Ecole normale supérieure, PSL Research University, UPMC Univ Paris 06, CNRS, Département de Chimie, PASTEUR, 24, rue Lhomond, 75005 Paris, France. E-mail: frederic.lemaitre@ens.fr*
[b]*Sorbonne Universités, UPMC Univ Paris 06, ENS, CNRS, PASTEUR, 75005 Paris, France*
[c]*Laboratoire de physiologie membranaire et moléculaire du chloroplaste, CNRS, UPMC UMR 7141, I.B.PC., 13 rue Pierre et Marie Curie, 75005 Paris, France*

†Electronic supplementary information (ESI) available. See DOI: 10.1039/c6pp00076b

‡Current address: School of Chemistry, University of New South Wales, Sydney, NSW 2052, Australia.

§F. Rappaport died before completion of this manuscript. His co-authors wish to dedicate this article to his memory.

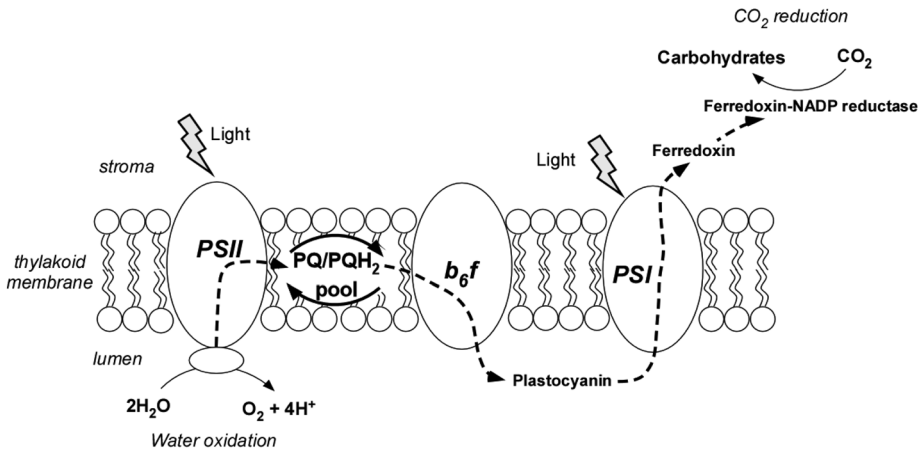

Fig. 1 Simplified scheme of photosynthesis in the thylakoid membrane. The dashed line traces the endogenous electron flow along the photosynthetic electron transport chain. Abbreviations: Photosystems I and II (PSI and PSII), plastoquinone (PQ), plastoquinol (PQH_2), and cytochrome b_6f (b_6f).

For instance, thylakoid membranes can be immobilized on a working electrode in order to perform a direct electron transfer.[3,4] In that case, by using a redox polymer, nanoparticles or nanotubes has been demonstrated to help the photosynthetic electrons to shuttle from the photosynthetic chain to the electrode.[5–7] Alternatively, isolated photosystems can be grafted on the electrode surface. Here again, the electron transfer could be achieved through conducting or redox polymers.[8–11] It is worth mentioning that photocurrent production from photosynthesis is not restricted to isolated photosynthetic units. For example, promising photocurrents can also be obtained with intact biological systems like cyanobacteria[12–16] or green algae.[17] It has to be also emphasized that using more complex systems like plants has recently been considered as an encouraging approach.[18,19]

Among all these strategies, exogenous redox mediators can be subsequently engaged as electron carriers to improve the electron transfer, thus giving rise to higher current densities. Hence, the oxidised form would be devoted to short-circuiting the electron transfer by extracting the electrons, while its reduced form would deliver them by their oxidation at the electrode surface. Within this context, exogenous quinones are often used to enhance the extraction of photosynthetic electrons from isolated thylakoid membranes[5] as well as from intact cells.[20–23] In a previous study based on fluorescence measurements, we characterized the ability of several quinones to extract photosynthetic electrons from Photosystem II (PSII) in a mutant strain of *Chlamydomonas reinhardtii* which lacks the cytochrome b_6f complexes (b_6f mutant), thus being inefficient in utilizing electrons photoproduced by Photosystem II.[24] We estimated the extraction efficiency of several exogenous quinones and provided evidence for a limitation in the availability of quinones due to their partition between intracellular membranes and other aqueous compartments. In the present work, we further analyze the effect of light intensity and quinone concentration with respect to our modeling of extraction of photosynthetic electrons using exogenous quinones. This led us to establish a zone diagram aimed at defining the most appropriate experimental conditions to extract photoelectrons from intact algae according to the purpose of the study.

Results and discussion

PSII-controlled fluorescence changes were monitored in a suspension of *Chlamydomonas reinhardtii* cells from a mutant, Δ*petA*, which lacks the b_6f complex.[24] Several quinones (1,4-benzoquinone (BQ), 1,4-naphthoquinone (NQ), 2,6-dichlorobenzoquinone (2,6-DCBQ), 2,5-dichlorobenzoquinone (2,5-DCBQ), 2,6-dimethylbenzoquinone (2,6-DMBQ), 2,5-dimethylbenzoquinone (2,5-DMBQ), *p*-phenylbenzoquinone (PPBQ)) were thus benchmarked for their capability to extract electrons downstream of Photosystem II. However, both the effect of quinone concentration and that of light intensity on the efficiency of electron extraction needs to be carefully assessed in order to better understand the mechanism and set up appropriate conditions for future electrochemical harvesting. To this end, we used fluorescence experiments to determine the proportion of open reaction centers (Fig. 2).[24] Briefly, an open Photosystem II reaction center corresponds to a moiety in which the primary quinone electron acceptor Q_A is in its oxidized state (Fig. 3).[25] Therefore, it can be involved in a charge separation. Conversely, a closed reaction center is related to structures where Q_A is reduced to Q_A^- (Fig. 3). The open center ratio (defined here as Φ) can be calculated from the fluorescence measurements using eqn (1):[24,26]

$$\Phi = \frac{F'_{max} - F'_{stat}}{F'_{max} - F'_0} \quad (1)$$

It is worth mentioning that Φ is a good proxy for evaluating the ability of a given exogenous quinone to remove electrons from Q_A^-. Thus, the more efficient the extraction the closer to 1 are Φ values.

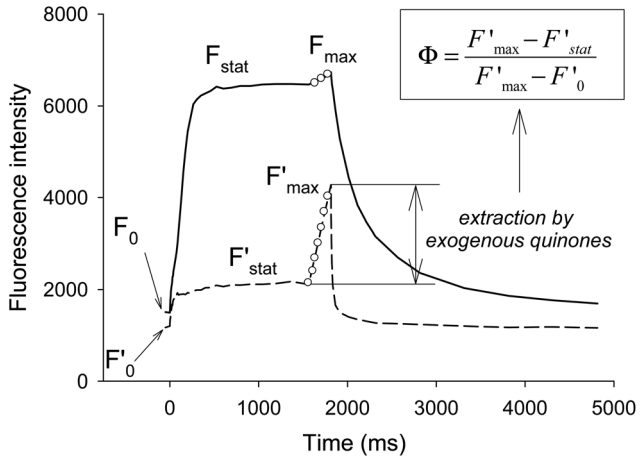

Fig. 2 A typical fluorescence experiment demonstrating the photosynthetic electron extraction by exogenous quinones on mutant algae at I° = 135 μE m^{-2} s^{-1} without any exogenous quinone (solid line) or in the presence of 2,6-DCBQ (30 μM, dashed line). The fluorescence decrease (F_{stat} to F'_{stat}) is due to quenching and extraction by the exogenous quinone. A subsequent supersaturating light pulse rapidly closes all open centers, which can not be reopened by the exogenous quinones, leading to a fluorescence increase (F'_{stat} to F'_{max}), allowing one to discriminate the fluorescence variations induced by quenching and extraction phenomena. In that way, the open reaction center ratio can be deduced. Because no data were recorded during the saturated pulse (F_{max} is only measured after the saturating pulse, see the Experimental part), the discontinuity is indicated by open circles.

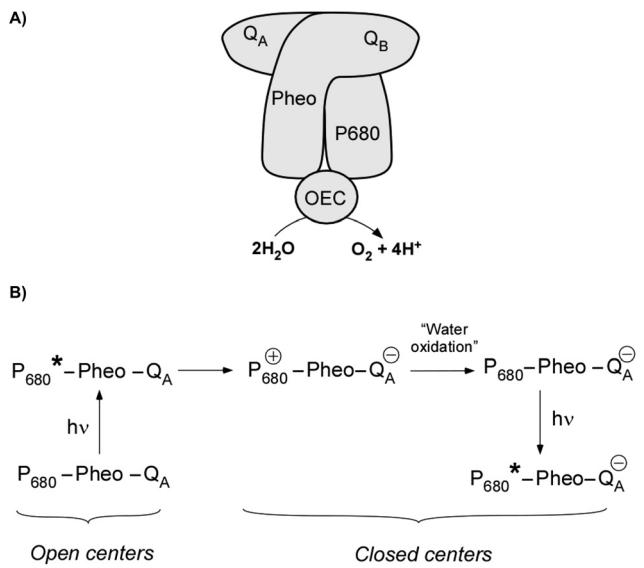

Fig. 3 (A) Simplified scheme of electron transfers occurring in Photosystem II to the plastoquinone pool. After excitation, the reaction center P680 induces water oxidation by the Oxygen Evolving Complex (OEC). P680 also reduces the primary acceptor Q_A by way of pheophytin (pheo). The electron is then transferred to a plastoquinone (PQ) bound in the Q_B pocket. (B) Scheme of open and closed centers of Photosystem II after a proper excitation of P680.

Light intensity effect on the electron extraction by exogenous quinones

Fluorescence experiments were performed using an exogenous quinone (2,6-DCBQ) whose ability to accept photosynthetic electrons was previously established.[24] Variations in the open center ratio can be displayed as a function of the available quinone concentration, C_Q (*i.e.* the difference between the introduced quinone concentration and the sequestered one in other cell compartments; see ref. 24 for more details) for five light intensities (56, 135, 340, 800 and 1500 μE m^{-2} s^{-1}; see Fig. 4).

As expected, the open center ratio, and thus the electron extraction, strongly depends on the light intensity. Expectedly, it significantly increases with decreasing light intensity since Φ can be viewed as a yield resulting from two opposite reactions occurring during the illumination, *i.e.* the light-induced formation of closed reaction centers through the Q_A reduction and their reoxidation by exogenous (or endogenous) quinones. Therefore, a higher incident light will increase the number of closed reaction centers and thus decrease Φ values. By considering that the extraction yield corresponds to Michaelis–Menten like kinetics, all the graphs displaying Φ as a function of C_Q can be fitted and show good agreement with the following equation:

$$\Phi = \frac{\Phi_0 \dfrac{\Phi_\infty}{\rho_0} + \Phi_\infty C_Q}{\dfrac{\Phi_\infty}{\rho_0} + C_Q} \qquad (2)$$

Considering Fig. 4, Φ_∞ is the open center ratio value reached at infinite quinone concentration and ρ_0 the initial slope of the exogenous flow part of the curve displaying Φ as a function of C_Q. It has to be emphasized that despite the absence of the b_6f complex in the mutant investigated here, a residual endogenous electron flux can still occur.[24] As a consequence, the open reaction center ratio is not zero in the absence of exogenous quinones (particularly at low excitation intensities[24]) and the corresponding value will be defined as Φ_0. The values of Φ_0, Φ_∞ and ρ_0 can thus be extracted and are collected in Table 1.

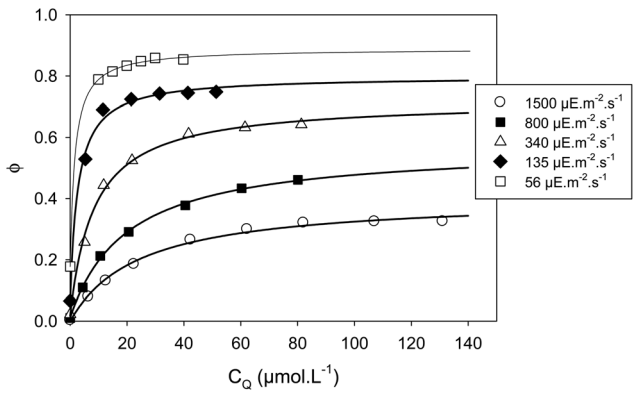

Fig. 4 Open center ratio Φ as a function of the available 2,6-DCBQ concentration C_Q for five light intensities (56, 135, 340, 800 and 1500 μE m^{-2} s^{-1}).

Table 1 Effect of the light intensity I^o on the extracted values reflecting the electron extraction induced by the exogenous 2,6-DCBQ addition (Φ_∞ and ρ_0) and the open center ratio in the absence of exogenous quinones (Φ_0) for mutant algae

I^o (μE m^{-2} s^{-1})	Φ_∞	ρ_0 (μmol^{-1} L)	Φ_0
1500	0.38 ± 0.01	$(1.9 \pm 0.3) \times 10^{-2}$	$(3.4 \pm 2.0) \times 10^{-3}$
800	0.58 ± 0.01	$(2.7 \pm 0.1) \times 10^{-2}$	$(1.0 \pm 0.1) \times 10^{-2}$
340	0.71 ± 0.01	$(9.0 \pm 0.5) \times 10^{-2}$	$(2.2 \pm 0.3) \times 10^{-2}$
135	0.77 ± 0.01	$(5.4 \pm 0.1) \times 10^{-1}$	$(6.6 \pm 0.2) \times 10^{-2}$
56	0.89 ± 0.19	$(4.9 \pm 0.9) \times 10^{-1}$	0.18 ± 0.03

Because Φ_0 is the open center ratio in the absence of exogenous quinones under a given irradiation, it corresponds to the endogenous flow yield for the PSII acceptor reoxidation. When Φ_0 is close to 0 there are no open centers, meaning that the closed center reoxidation rate due to the endogenous flow is lower than the open center reduction rate due to irradiation. Conversely, if Φ_0 is close to 1, there are no closed centers, meaning that the open center reduction kinetics due to irradiation is much slower than the closed center reoxidation kinetics due to the endogenous flow. Table 1 indicates very low Φ_0 values according to the absence of the b_6f complex in the mutant (see above). Moreover, the light intensity alters the Φ_0 values. The higher the incident light the lower the Φ_0 values in agreement with an increased number of closed centers due to the illumination.

Because Φ_∞ is the maximum open center ratio under a given irradiation, it corresponds to the maximum exogenous flow yield for the PSII acceptor reoxidation under the irradiation conditions. When Φ_∞ is close to 1, the open center reduction rate due to irradiation is much lower than the closed center reoxidation rate due to the exogenous flow, which is one of the features of an efficient extraction. The opposite comparison is made when Φ_∞ is close to 0. ρ_0 corresponds to the slope from Φ_0 to Φ_∞ and also allows us to assess the electron extraction. A ρ_0 value close to 0 will lead to a Φ value close to Φ_0, *i.e.* in the case in which no extraction occurs even with a high exogenous quinone concentration. Conversely, when $\rho_0 \to \infty$, the Φ value will be close to its maximum Φ_∞ value, thus leading to a situation where even rather low exogenous concentrations lead to an efficient extraction. Both Φ_∞ and ρ_0 values also decrease with increasing light intensity, in accordance with a reduced number of open centers due to a more intense illumination. Finally, the extraction efficiency can be modified by means of the quinone concentration or light intensity. We found no experimental condition that would preserve a full oxidation of PSII centers, even at high quinone concentration. This thus raises the question of the most appropriate conditions for performing harvesting of photosynthetic electrons.

Definition of a mechanism for electron extraction by exogenous quinones

In order to use our experimental data to predict the most adapted conditions of extraction, we propose to consider the simple mechanism depicted in Fig. 5. Q_A^- is viewed as the main target of exogenous quinones that would compete with the natural plastoquinone secondary acceptor within the Q_B pocket.[27–33] Due to the high affinity for the quinones investigated in this work (DCBQ and PPBQ, see below) with the Q_B pocket,[31,34–36] an electron exchange between the exogenous quinone and the plastoquinone pool will not be considered in the mechanism proposed here, but it cannot be totally excluded.

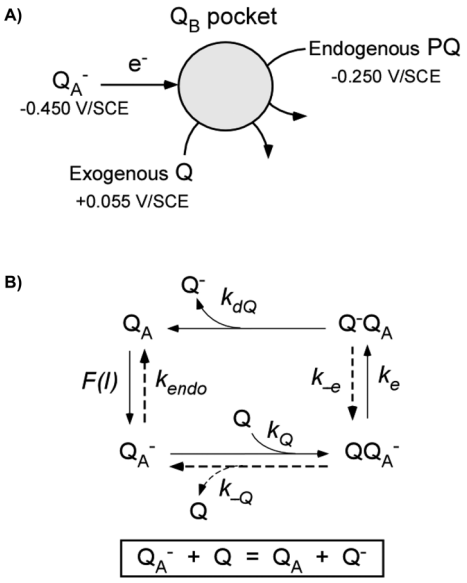

Fig. 5 (A) Scheme showing competition for photosynthetic electrons between the exogenous quinone Q and the endogenous PQ. The mid-potential values are given for Q_A, Q (in the case of 2,6-DCBQ) and PQ. (B) Detailed representation of the suggested extraction mechanism.

Therefore, the proposed model is based on the electronic transfer between Q_A^- and the exogenous quinone Q according to:

$$Q_A^- + Q = Q_A + Q^- \quad (3)$$

The extraction process shown in Fig. 5B is described in the following manner. First of all, after illumination, the photo-induced charge separation leads to the formation of closed reaction centers Q_A^- (with an incident light dependent rate constant $F(I)$). The closed center Q_A^- can then react in two different pathways. On the one hand, Q_A^- can be reoxidised through the endogenous electron flow occurring in the photosynthetic chain (with a rate constant k_{endo}). On the other hand, Q_A^- can interact with the exogenous quinone Q to lead to an electron transfer. Such an electron transfer requires two equilibrated steps: the reversible binding of the exogenous quinone Q within the pocket (k_Q and k_{-Q} are the forward and backward rate constants, respectively, from the Q insertion within the Q_B pocket) and the electron transfer itself between Q_A^- and Q (k_e and k_{-e} are the forward and backward electron transfer rate constants, respectively, from Q_A to the bound exogenous quinone Q; due to the significant difference between E^o values for Q and Q_A^- (see below), k_e is expected to be larger than k_{-e}).

The final step is the irreversible extraction due to the release of the reduced form of the exogenous quinone from the Q_B pocket (rate constant k_{dQ}). The reoxidation of Q_A^- into Q_A involving the exogenous quinone Q through these three successive steps will now be referred to as the exogenous flow.

At this stage, it should be pointed out that this simple one electron mechanism may give a limited scope for the whole extraction process since quinones correspond to bielectronic systems. This question will be addressed more thoroughly in a later section and the ESI† and only the simple one electron mechanism will be considered.

Assuming that the open center ratio is constant when steady state fluorescence is reached, one can consider the ratios of the four redox states involved here (Q_A, Q_A^-, QQ_A^- and Q^-Q_A) to be constant. Therefore applying the quasi steady state approximation to Q_A^-, QQ_A^- and Q^-Q_A, where the inputs and outputs of each state are equal, one has:

$$F(I)[Q_A] + k_{-Q}[QQ_A^-] = (k_{endo} + C_Q k_Q)[Q_A^-] \quad (4)$$

$$k_{-e}[Q^-Q_A] + k_Q C_Q[Q_A^-] = (k_e + k_{-Q})[QQ_A^-] \quad (5)$$

$$k_e[QQ_A^-] = (k_{-e} + k_{dQ})[Q^-Q_A] \quad (6)$$

The conservation of matter leads to:

$$[Q_A] + [Q_A^-] + [QQ_A^-] + [Q^-Q_A] = 1 \quad (7)$$

Finally, considering the open center ratio as the Q_A proportion, eqn (4)–(7) give eqn (8) (see details in the ESI†):

$$\Phi = [Q_A] = \frac{k_{endo}(k_{-Q}(k_{-e} + k_{dQ}) + k_{dQ}k_e) + k_Q k_{dQ} k_e C_Q}{(k_{endo} + F(I))(k_{-Q}(k_{-e} + k_{dQ}) + k_{dQ}k_e) + k_Q C_Q(F(I)(k_e + k_{-e} + k_{dQ}) + k_{dQ}k_e)} \quad (8)$$

Experimental validation of the mechanism with 2,6-DCBQ

Before considering the model as a tool to define the effects of experimental conditions on the photosynthetic electron extraction, the mechanism described above has to be validated by the experimental results. As described above, without any exogenous quinones ($C_Q = 0$), Φ should be equal to Φ_0. Therefore eqn (8) becomes:

$$\Phi = \Phi_0 = \frac{k_{endo}(k_{-Q}(k_{-e} + k_{dQ}) + k_{dQ}k_e)}{(k_{endo} + F(I))(k_{-Q}(k_{-e} + k_{dQ}) + k_{dQ}k_e)} = \frac{k_{endo}}{k_{endo} + F(I)} \quad (9)$$

Therefore, one has:

$$\frac{1}{\Phi_0} = 1 + \frac{F(I)}{k_{endo}} \quad (10)$$

The mechanism leads to a linear relationship between the inverse of the open reaction center ratio in the absence of exogenous quinones and the Q_A photoreduction rate constant $F(I)$ with an intercept with the y-axis equal to 1. As displayed in Fig. 6, $1/\Phi_0$ values as a function of the incident light flow $I°$ correspond to a straight line ($1/\Phi_0 = 1.1 \times 10^{-1} I° + 1$; $R^2 = 0.996$; the value at 1500 μE m^{-2} s^{-1} is not taken into account due to a too low Φ_0 value that leads to a high uncertainty). Beyond a first consistent result with the mechanism envisioned here, it suggests that $F(I)$ linearly depends on the incident light flux, and thus that Q_A reduction is controlled by light absorption and not by an intermediate step rate.

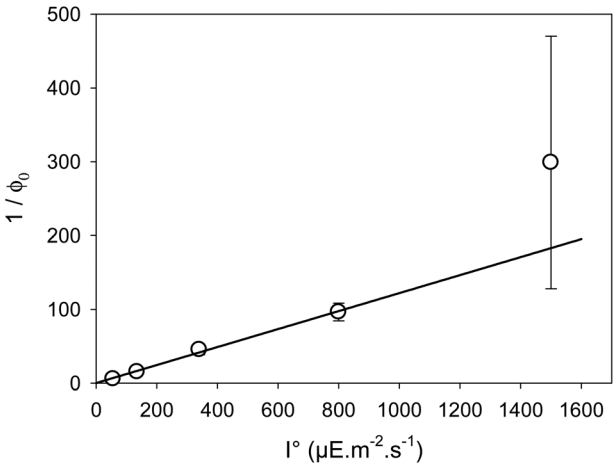

Fig. 6 Inverse of the open reaction center ratio in the absence of exogenous quinones ($1/\Phi_0$) as a function of the incident light intensity for mutant algae.

Another way to validate the mechanism of electron harvesting by exogenous quinones is to consider Φ_∞ values. Hence, as already defined, Φ_∞ mathematically corresponds to Φ values at infinite quinone concentrations. So eqn (8) becomes:

$$\Phi = \Phi_\infty = \frac{k_{dQ}k_e}{F(I)(k_e + k_{-e} + k_{dQ}) + k_{dQ}k_e} \quad (11)$$

Therefore, one has:

$$\frac{1}{\Phi_\infty} = 1 + \frac{F(I)(k_e + k_{-e} + k_{dQ})}{k_{dQ}k_e} \quad (12)$$

As displayed in Fig. 7, eqn (12) is consistent with experimental results ($1/\Phi_\infty = 1 + 1.1 \times 10^{-3} I°$; $R^2 = 0.996$). It is worth mentioning that similar experiments with wild type algae were also achieved (see Fig. 7 and S1 in the ESI†). In this case, the slope did not significantly change (1.2×10^{-3} m^2 s μE^{-1}) as expected. Indeed, wild type and b_6f mutant only differ in terms of endogenous electron flux. Since eqn (12) shows that the $1/\Phi_\infty$ does not depend on k_{endo}, the slope values of the $1/\Phi_\infty = f(I°)$ graphs are expected to be similar regardless of the considered algae.

Additionally, eqn (12) suggests that, following the rate limiting step at infinite quinone concentrations, the Φ_∞ value may be correlated to the electron transfer rate constant k_e. As a con-

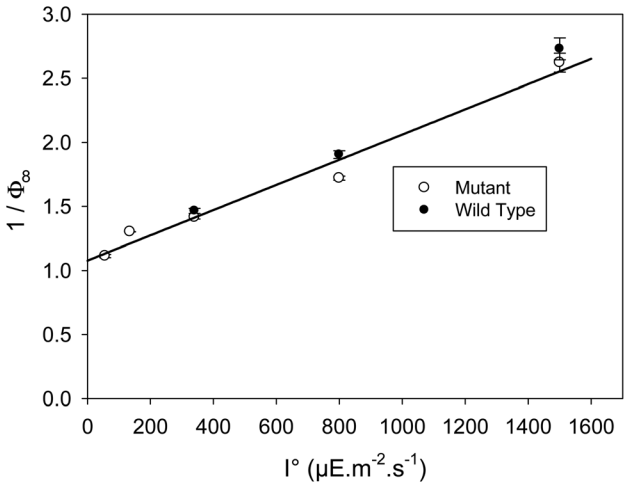

Fig. 7 Inverse of the maximum open reaction center ratio ($1/\Phi_\infty$) as a function of the incident light intensity in the presence of 2,6-DCBQ for mutant (white circles) and wild-type (filled circles) algae.

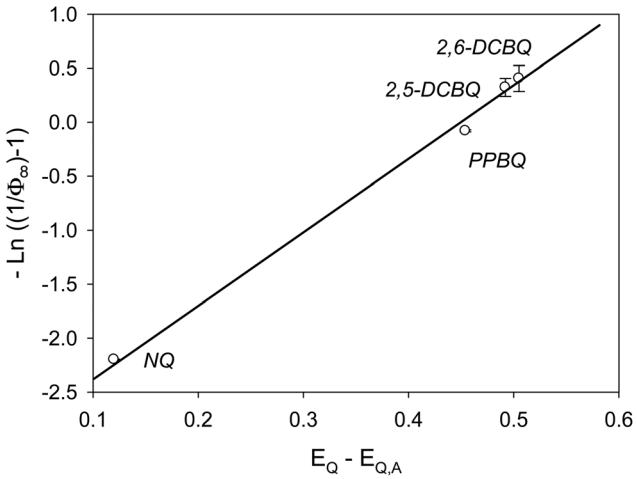

Fig. 8 $\ln((1/\Phi_\infty) - 1)$ parameter as a function of the $E_Q - E_{QA}$ term (see the text) for experiments ($I°$ = 340 μE m^{-2} s^{-1}) involving four exogenous quinones (NQ, PPBQ, 2,5-DCBQ and 2,6-DCBQ).

sequence, it could be correlated with the difference of standard potentials between the exogenous quinone and Photosystem II reduced electron acceptor Q_A^-. Indeed, according to the molecular electron transfer rate law related to Marcus theory, a quadratic dependence of the rate constant logarithm as a Gibbs free energy function (which can be assumed as the reaction driving force) is expected, as shown in eqn (13).

$$\log(k_e) = \log(k_e^{\Delta_r G°=0}) - \frac{\Delta_r G°}{2RT} - \frac{(\Delta_r G°)^2}{4\lambda RT} \quad (13)$$

λ is the system reorganization energy, which corresponds to the energy which would have to be provided to put the reactant into the product configuration (bond length, solvation conditions, *etc.*). Moreover, eqn (12) leads to:

$$-\ln\left(\frac{1}{\Phi_\infty} - 1\right) = -\ln\left(\frac{F(I)(k_e + k_{-e} + k_{dQ})}{k_{dQ}}\right) + \ln(k_e) \quad (14)$$

Fig. 8 displays the $(-\ln((1/\Phi_\infty) - 1)$ parameter as a function of the difference of standard potentials between the exogenous quinone (E_Q) and electron acceptor Q_A^- (E_{QA}) for four quinones. Briefly, all the data treatments (extracted values of Φ_∞ at $I°$ = 340 μE m^{-2} s^{-1}) described above were performed for four quinones (NQ, PPBQ, 2,6-DCBQ and 2,5-DCBQ) and the standard potentials were extracted from previous studies (+0.042; +0.055; +0.004; −0.330 V *vs.* SCE (Saturated Calomel Electrode) for the exogenous quinones respectively and −0.450 V *vs.* SCE for Q_A^-).[24,37] Interestingly, Fig. 8 suggests a linear relationship instead of the expected parabolic curve. In that case, the quadratic term in eqn (13) would be much lower than $0.5\Delta_r G°/RT$, thus meaning that the reorganization energy would be much higher than the driving forces investigated here. While a deeper analysis with other quinones involved in the mechanism considered in this work should be made to confirm this trend, such a behavior could be explained if assuming high reorganization energy. Indeed, due to altered interactions between quinones and proteins by the electron transfer, the resulting local protein structure reorganization in a confined environment should be more energy consuming than a usual solvation sphere.

Consequently, our results support the mechanism suggested in Fig. 5 (complementary validations are reported in the ESI, see Fig. S2 and S4†). It is worthy of note that it does not fully exclude alternative mechanisms (see below). Moreover, the Φ_∞ values seem to be controlled by an electron transfer rate law, meaning that the Q^-Q_A dissociation should be much faster than the electron transfer step.

Beyond the fact that our mechanism is validated by the experimental results, only considering one accepted electron by exogenous quinones needs to be discussed because the resulting semiquinone Q^- should not leave easily the Q_B pocket. Therefore, a second electron should be accumulated leading to a final quinol species. Owing to the high affinity of quinones for the Q_B pocket,[31] an alternative mechanism with two successive electron transfer steps can be proposed similar to the plastoquinone reduction. All the corresponding equations are detailed in the ESI.† Indeed, despite much more complicated equations, such a bielectronic extraction mechanism also allows one to describe the effects of experimental conditions ($I°$, C_Q) on the quantities (Φ; Φ_∞; Φ_0; ρ_0) related to the extraction. On the one hand, it means that the intrinsic properties resulting from a two electron mechanism cannot be detected in the ranges of experimental conditions and sensitivity we have considered in the present work. On the other hand, it especially means that applying a simple monoelectronic extraction to our results is adequate to build zone diagrams able to predict the most appropriate conditions and to give access to the zones in which the rate limiting step depends on the quinone concentration (quinone binding into the Q_B pocket) or not.

Zone diagram for deeper analysis of the extraction mechanism

Predicting the effect of quinone concentration and light intensity on the photosynthetic electron extraction requires understanding the consequences of the model described here and more particularly the different steps that limit the whole process.

Thus, following the different rate constants in the mechanism (endogenous flow, electron transfer, *etc.*) or the different experimental parameters (quinone concentration and incident light flow), the open center ratio will not be controlled by the same flow (endogenous *vs.* exogenous). Moreover, the rate determining step of exogenous flow may also differ (electron transfer *vs.* quinone insertion). That is why we first sought to build a general zone diagram to summarize prominent flows and rate limiting steps as a function of the different rate constants and experimental parameters. To do so, one has to consider the expression of the open center ratio in eqn (8). Considering that the presence of exogenous quinones induces a corresponding electron flow, the ratio between the exogenous (due to C_Q) flow (J_{exo}) and endogenous electron (due to k_{endo}) flow (J_{exo}) is defined as α according to (see details in the ESI†):

$$\alpha = \frac{J_{exo}}{J_{endo}} = C_Q \frac{k_Q k_{dQ} k_e}{k_{endo}(k_{-Q}k_{-e} + k_{-Q}k_{dQ} + k_{dQ}k_e)} \quad (15)$$

Therefore, the adimensional parameter α notably depends on the quinone concentration C_Q whose value will directly play a significant role in the prevalent flow. For instance, if $\alpha > 1$, the exogenous flux will predominate.

Moreover, considering eqn (15), eqn (8) becomes:

$$\Phi = \frac{k_{endo}(1+\alpha)}{(k_{endo} + F(I)) + \alpha k_{endo}\left(\frac{F(I)(k_e + k_{-e} + k_{dQ})}{k_{dQ}k_e} + 1\right)} \quad (16)$$

Furthermore, as displayed in Fig. 5B, the available quinone concentration (C_Q) will only modify the quinone insertion rate. As a consequence, the exogenous flow can be rate-determined either by the exogenous quinone Q arrival within the Q_B pocket or the subsequent electron transfer between Q and Q_A. The prevalence of each is thus related to the comparison between the quinone concentration dependent and independent terms of the denominator in eqn (8). A second adimensional parameter β can be defined as follows:

$$\beta = \frac{k_{endo} + F(I)}{k_{endo}\left(\frac{F(I)(k_e + k_{-e} + k_{dQ})}{k_{dQ}k_e} + 1\right)} \quad (17)$$

β corresponds to a specific α value for which quinone insertion and electron transfer rates are equal. The electron transfer rate will be much higher than the insertion if $\alpha \ll \beta$, thus leading to the quinone insertion as the rate determining step. Eqn (16) finally becomes:

$$\Phi = \frac{k_{endo}(1+\alpha)\beta}{(k_{endo} + F(I))(\alpha + \beta)} = \Phi_0 \frac{(1+\alpha)\beta}{\alpha + \beta} \quad (18)$$

The corresponding zone diagram is depicted in Fig. 9. Such a diagram illustrates how the open center ratio depends on the quinone concentration in a specific manner related to the prevalence of electron fluxes and kinetics. The yellow line splits the diagrams into two zones related to β values, *i.e.* a normal region for $\beta > 1$ (that leads to a Φ increasing function) and an inverted region for $\beta < 1$ (that leads to a Φ decreasing function). Comparing α value to 1 and α value to β allows one to define 9 main zones corresponding to a specific dependence of Φ towards C_Q, as listed in Table 2.

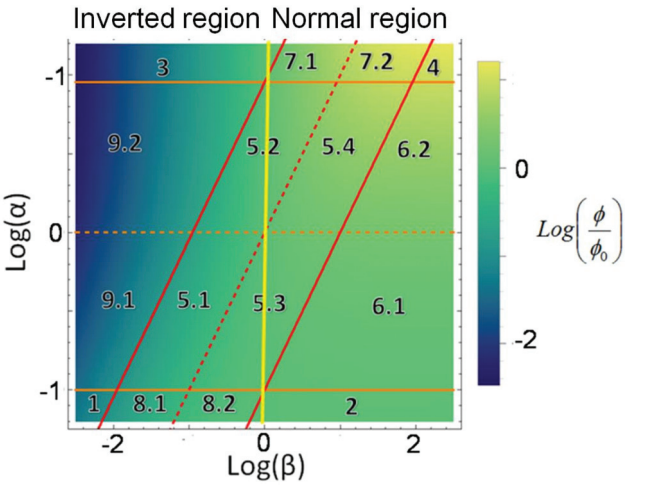

Fig. 9 Zone diagram of the open center ratio as a function of α and β parameters (see the text). The vertical yellow line corresponds to the frontier between inverted ($\beta < 1$) and normal ($\beta > 1$) regions. Nine main zones (1–9) were thus defined considering red and orange solid lines. Orange solid lines correspond to frontiers from which one of the fluxes can be neglected (less than 10%). Red solid lines correspond to frontiers from which fluxes can be simplified by neglecting one of the kinetics limitations. Dashed lines allow one to define sub-zones. The dashed orange line corresponds to equal endogenous and exogenous fluxes. The red dashed line is related to conditions for which the exogenous flux is equally both rate-determined by electron transfer and the quinone arrival.

In particular, eqn (17) shows that the transition between inverted and normal regions is based on the $k_{endo}(k_e + k_{-e} + k_{dQ})/(k_{dQ}k_e)$ value. If $k_{endo} < (k_{dQ}k_e)/(k_e + k_{-e} + k_{dQ})$ (*i.e.* $\beta > 1$), the quinone addition and insertion leads to a state (QQ_A^-) that releases its charge faster than (Q_A^-) by endogenous flow. The open center ratio is thus expected to increase with the added quinone concentration. Conversely, if $k_{endo} > (k_{dQ}k_e)/(k_e + k_{-e} + k_{dQ})$ (*i.e.* $\beta < 1$), the back formation of Q_A from Q_A^- will be faster than the charge release of (QQ_A^-) accumulated when the quinone concentration increases.

The open center ratio is thus expected to decrease with the added quinone concentration. Such trends are readily observed in three inverted zones (1, 8, 9) and three normal zones (4, 6, 7). Finally, two peculiar zones (2 and 3) are independent of the quinone concentration. Indeed, if the endogenous flow prevails with a limiting quinone transport (zone 2), the quinone insertion is prevented by the back formation of Q_A. Therefore, no significant extraction by the exogenous quinone can occur and the resulting open center ratio will be close to its value in the absence of quinone. Conversely, if the

Table 2 Summary of the effects on the open center ratio of α (endogenous *vs*. exogenous flows) and β (electron transfer *vs*. quinone transport kinetics) values

Zone	Prevalent flow	Exogenous flow r.d.s	Φ	Dependence on quinone concentration?	Region
1	Endogenous ($\alpha < 1$)	Electron transfer ($\beta < \alpha$)	$\Phi = \Phi_0 \frac{\beta}{\alpha} = \frac{\Phi_0 \Phi_\infty}{\rho_0} \frac{1}{C_Q}$	Yes, decreasing function	Inverted
2	Endogenous ($\alpha < 1$)	Mass transport ($\beta > \alpha$)	$\Phi = \Phi_0$	No	Mainly normal
3	Exogenous ($\alpha > 1$)	Electron transfer ($\beta < \alpha$)	$\Phi = \Phi_0 \beta = \Phi_\infty$	No	Mainly inverted
4	Exogenous ($\alpha > 1$)	Mass transport ($\beta > \alpha$)	$\Phi = \Phi_0 \alpha = \rho_0 C_Q$	Yes, increasing function	Normal
5	Both	None	$\Phi = \Phi_0 \frac{(1+\alpha)\beta}{(\alpha+\beta)}$	Yes	Both
6	Both	Mass transport ($\beta > \alpha$)	$\Phi = \Phi_0 \frac{(1+\alpha)\beta}{\beta} = \Phi_0 + \rho_0 C_Q$	Yes, increasing function	Normal
7	Exogenous ($\alpha > 1$)	None	$\Phi = \Phi_0 \frac{\alpha\beta}{(\alpha+\beta)} = \frac{\Phi_\infty C_Q}{\frac{\Phi_\infty}{\rho_0} + C_Q}$	Yes, increasing function	Normal
8	Endogenous ($\alpha < 1$)	None	$\Phi = \Phi_0 \frac{\beta}{(\alpha+\beta)} = \frac{\Phi_0 \Phi_\infty}{\Phi_\infty + \rho_0 C_Q}$	Yes, decreasing function	Inverted
9	Both	Electron transfer ($\beta < \alpha$)	$\Phi = \Phi_0 \frac{(1+\alpha)\beta}{\alpha} = \Phi_\infty + \frac{\Phi_\infty \Phi_0}{\rho_0} \frac{1}{C_Q}$	Yes, decreasing function	Inverted

exogenous flux prevails with a limiting electron transfer step (zone 3), the quinone insertion is a very fast step. On the one hand, the extraction rate does not depend on C_Q and, on the other hand, the open center ratio will reach its maximum value (Φ_∞) under the irradiation conditions.

It is worth mentioning that the inverted region corresponds to a counter-intuitive behavior because increasing the exogenous quinone concentration decreases the open center ratio. In other words, the inverted region corresponds to conditions under which adding an oxidant leads to a more reduced system. Hence, another way to validate the suggested mechanism is to experimentally demonstrate that the inverted region exists. The established zone diagram shows that it can be achieved by considering another system (quinone/algae) whose electron transfer kinetics (step generating (Q^-Q_A) from (QQ^-_A)) is rather low compared to endogenous flow (direct back generation of Q_A starting from Q_A^-). Experiments were thus carried out with 2,6-DCBQ with wild-type algae for which the endogenous flow is expected to be larger (the photosynthetic chain is complete, thus the endogenous flow rate constant k_{endo} is higher than the mutant one). Nevertheless, increasing the quinone concentration still leads to the increase of the open center ratio (see Fig. S3 and Table T1 in the ESI†), thus meaning that experimental conditions still correspond to the normal region of the diagram because the endogenous flow, although much stronger than in the mutant case, remains slower than electron transfer to 2,6-DCBQ.

As a consequence, other experiments were still performed with wild-type algae but in the presence of an electron PSII acceptor, naphthoquinone (NQ), which was previously demonstrated to be limited by a low Φ_∞ value. Such a result is consistent with its low midpotential value,[24] which suggests a slow electron transfer after binding within the Q_B pocket. Hence, applying the experiments and data treatment with the population of b_6f mutant or wild type algae gives the $\Phi = f(C_Q)$ depicted in Fig. 10 and corresponds to the expected poor reductive capability of NQ. In the mutant case, the open center ratio is still an increasing function because, although the electron transfer is also slow, the endogenous flow is slower. However, in the wild type case, the electron transfer step is not only slow but also takes place in the presence of an initial significant endogenous flow. Therefore exogenous quinone addition will short-circuit the endogenous flow and lead to an accumulation of closed reaction centers (QQ_A^-), thus resulting in a decrease of Φ as a function of quinone concentration. That is why the inverted region of the diagram was reached for such experimental conditions, thus strengthening the extraction mechanism investigated here and its use for predicting the effects of the added quinone concentration and the light intensity.

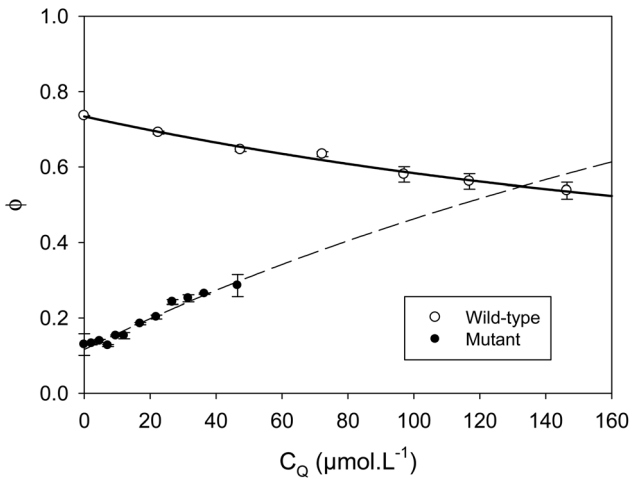

Fig. 10 Open center ratio Φ as a function of the available NQ concentration C_Q ($I°$ = 135 µE m^{-2} s^{-1}) in the case of wild-type algae (white circles) and mutant algae (filled circles).

Building a zone diagram for deciphering the effects of quinone concentration and light intensity

In order to predict the effect of quinone concentration and light intensity on the photosynthetic electron extraction, another zone diagram can be built owing to the experimentally extracted values of Φ_0, ρ_0 and Φ_∞ for 2,6-DCBQ and the mutant without b_6f. Hence, the Φ values can be predicted by means of eqn (2) for the light intensities investigated in the present work. Such results can then be used to build a new zone diagram that will display the effect of quinone concentration and light intensity on the open center ratio value (see Fig. 11 for the mutant case; a similar diagram can be built for the wild-type case, see Fig. S5 in the ESI†). First of all, some of the inverted regions described in Fig. 9 (corresponding to zones 1, 8, 9) cannot be observed. Indeed, experimental data showed that the open center ratio globally increased with the quinone concentration. It means that $\beta > 1$ in the 2,6-DCBQ case. This prevents direct observation of inverted zones and suggests that the electron transfer between the exogenous quinone and Q_A^- is faster than the endogenous flow. It is worth mentioning that observation of inverted zones is quinone and algae dependent, and quinone concentration and light intensity independent. Indeed, the above experiments involving NQ with wild-type algae have shown a decrease of Φ while increasing C_Q, thus featuring an inverted behavior with $\beta < 1$.

Hence, among all the zones within or crossing the inverted region (see Fig. 9), only zones 2, 3, and 5 are still observed. Finally, as mentioned above, all the normal zones are observed excepting zone 4 (where exogenous flow predominates and mass transport is rate-determining). The absence of zone 4 is consistent with the fact that when exogenous flux controls the open center ratio, the electron transfer kinetics limitation cannot be neglected. Indeed, assuming that a term can be neglected in a sum if it is less than 10% of the other terms, such a zone corresponds to $\beta > 100$ because exogenous flow is assumed to predominate ($\alpha > 10$) with a mass transport limitation ($\beta > 10\alpha$). In other words, it would require that QQ_A^- release its charge at least 100 times faster than Q_A^- with endogenous flow. So the higher the difference between β and 100, the bigger the zone 4 area. According to eqn (9), (11) and (17), β can be calculated as:

$$\beta = \frac{\frac{1}{\Phi_0} - 1}{\frac{1}{\Phi_\infty} - 1} \tag{19}$$

By using the previously extracted slopes, a β value equal to 100 is obtained. These peculiar conditions being just below the threshold of zone 4 existence, zone 4 is therefore not observed. Beyond the mapping of the open center ratio, such a zone diagram can help to identify specific experimental conditions for photosynthetic electron extraction.

More particularly, such a diagram allows us to predict the effects of exogenous quinone concentration at a given incident light. Very low quinone concentrations lead to experimental conditions corresponding to zone 2. This case ($\Phi = \Phi_0$) is obviously not suitable because, according to the biological redox state sensitivity, no significant extraction will occur. Conversely, working with a moderate exogenous quinone concentration will lead to experimental conditions defining zone 6 ($\Phi_0 = \Phi_0 + \rho_0 C_Q$) at high incident light. It thus allows one to extract the photosynthetic electrons without altering the endogenous flux. However, the open center ratio will not reach its maximum value (Φ_∞), thus it does not describe the optimal conditions to avoid photoinhibition. The best extraction can be obtained by working at high quinone concentrations, thus leading to experimental conditions corresponding to zone 3 ($\Phi = \Phi_\infty$). It allows one to perform electron extraction with the maximum efficiency at a given light intensity. That is why at a given incident light intensity, working at the frontier between zones 3 and 7 should provide interesting conditions since they would lead to the maximum Φ value with a quinone concentration kept as low as possible. The harvesting should thus be strongest while potentially reducing the damage resulting from photoinhibition. Nevertheless, because of the competition between endogenous and exogenous flows, increasing the electron extraction would drastically reduce the endogenous flow. It will therefore limit the NADPH formation which is also instrumental for algal viability.

Therefore, it is difficult to define the best zone for photosynthetic electron extraction. Indeed, one of the key points is the competition between endogenous and exogenous flows that are controlled by the light intensity and the exogenous quinone concentration. The choice should depend on the purpose of the investigation and the experimental conditions. Indeed, working without any energy source as an organic matter in the medium and maintaining algae alive for quite a long time should lead one to maintain a quite strong endogenous flow (and NADPH production). Zone 6 should thus be needed when working with relatively low quinone concentrations and moderate incident light. It would be optimal for

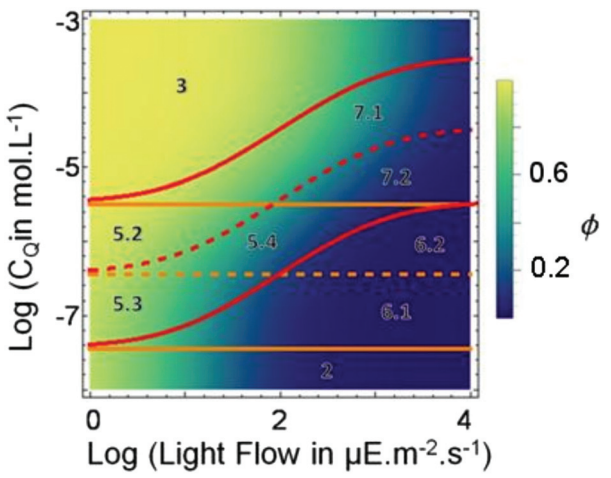

Fig. 11 Zone diagram of the open center ratio as a function of the quinone concentration C_Q and incident light $I°$. The frontier and the zone numbers are already defined in the legend of Fig. 9.

CO_2 consumption although the incident light flow should be carefully controlled because of possible photoinhibition during this extraction process. Moreover, a b_6f lacking mutant would not necessarily be the most appropriate system for such an investigation, due to its very low endogenous flow. Conversely, working to harvest photosynthetic electrons and produce maximum photocurrent values while also minimizing photoinhibition would require being at the frontier between zones 3 and 7. However, the system will not be totally efficient concerning the CO_2 reduction. Additionally, an organic matter source in the medium will be needed to preserve the algae lifetime.

Experimental

Cell culture and preparation

We used a wild type strain of *Chlamydomonas reinhardtii*, derived from 137c and a Δ*petA* mutant[38] that lacks cytochrome b_6f because of a deletion of the chloroplast gene encoding cytochrome f. Cytochrome b_6f is a quinol : plastocyanin oxidoreductase in the absence of which the plastoquinol generated by light-induced turnovers of Photosystem II cannot be re-oxidized, leading to the rapid arrest of light-driven electron flow. We characterized the respective ability of several distinct quinones to rescue a photoinduced electron flow in the mutant, using fluorescence to assess the Photosystem II photochemical rate.[25] Briefly, cells were grown in Tris Acetate Phosphate medium (TAP) containing Tris base (20 mmol L^{-1}), NH_4Cl (7 mmol L^{-1}), $MgSO_4$ (0.83 mmol L^{-1}), $CaCl_2$ (0.45 mmol L^{-1}), K_2HPO_4 (1.65 mmol L^{-1}), KH_2PO_4 (1.05 mmol L^{-1}) at 25 °C under moderate illumination (50 μE m^{-2} s^{-1}), centrifuged at 4000 rpm and then re-suspended into minimum medium (K_2HPO_4 (4.1 mmol L^{-1}), KH_2PO_4 (2.1 mmol L^{-1}), $CaCl_2$ (0.45 mmol L^{-1}), NH_4Cl (7.5 mmol L^{-1}), $MgSO_4$ (0.85 mmol L^{-1})) to a concentration of 10^7 cells per mL.

Preparation of chemical materials and solutions

All chemicals were purchased from Sigma Aldrich and used without any further purification. Quinones were dissolved in absolute ethanol in order to make stock solutions (typically 10 mmol L^{-1}). Appropriate small volumes of such quinone solutions were directly added into a cuvette containing the algae suspension (V = 2 mL) to achieve the final expected concentration. The cuvette was then stirred manually before experiments.

Fluorescence measurements and data acquisition

Fluorescence intensities were measured using a JTS spectrophotometer (Biologic) in which fluorescence was sampled with short flashes (4 μs duration) with negligible actinic (photobiological) effect. The detecting light for sampling fluorescence was provided by white LEDs and the wavelength (440 nm) defined by a combination of 3 mm BG39 and BG3 Schott filters. The open center ratio was calculated by means of the saturation pulse method (see the text).[25,39] The actinic (excitation) light was provided by a red LED (640 nm). This was used to promote excitation of PSII (continuous illumination with a steady state fluorescence F_{stat}, see light intensities in the text) and then induce a full reduction of the electron acceptors by means of a saturating pulse (5000 μE m^{-2} s^{-1}; 250 ms duration; fluorescence value F_{max} was measured to be 100 μs after the pulse was turned off; see the ESI†).[40,41]

Simulations and data treatment

Modeling and data treatment were performed using OriginPro 8.1 software (OriginLabcompany, Northampton, MA, USA) and Mathematica 9.0 student edition software (Wolfram Research Inc., Champaign, Illinois).

Conclusions

In this work we used fluorescence measurements to extract the open center ratio within a population of photosynthetic algae. Furthermore, we consider it as a proxy for investigating the extraction of photosynthetic electrons by means of an exogenous quinone, 2,6-DCBQ. A mechanism was suggested and was globally found consistent with the experimentally extracted parameters. Zone diagrams were constructed to identify the most appropriate experimental conditions (quinone concentration and light intensity) depending on the desired usage of the photosynthetic electron harvesting. As a consequence, it stresses the choice to preserve endogenous flow or to minimize photoinhibition and extract high photocurrent.

Acknowledgements

This work has been supported in part by CNRS (UMR 8640, UMR7141), Ecole Normale Supérieure, French Ministry of Research, Université Pierre & Marie Curie Paris 06, the "Fondation Pierre-Gilles de Gennes pour la Recherche" FPGG0049 and the "Initiative d'Excellence" program from the French State (Grant "DYNAMO", ANR-11-LABX-0011-01). Dr Benjamin Bailleul is also gratefully acknowledged for fruitful discussions.

Notes and references

1 R. E. Blankenship, D. M. Tiede, J. Barber, G. W. Brudvig, G. Fleming, M. Ghirardi, M. R. Gunner, W. Junge, D. M. Kramer, A. Melis, T. A. Moore, C. C. Moser, D. G. Nocera, A. J. Nozik, D. R. Ort, W. W. Parson, R. C. Prince and R. T. Sayre, *Science*, 2011, **332**, 805–809.
2 T. Roach and A. Krieger-Liszkay, *Curr. Protein Pept. Sci.*, 2014, **15**, 351–362.
3 M. Rasmussen and S. D. Minteer, *Electrochim. Acta*, 2014, **126**, 68–73.
4 M. Rasmussen and S. D. Minteer, *Phys. Chem. Chem. Phys.*, 2014, **16**, 17327–17331.
5 H. Hamidi, K. Hasan, S. C. Emek, Y. Dilgin, H.-E. Akerlund, P.-A. Albertsson, D. Leech and L. Gorton, *ChemSuschem*, 2015, **8**, 990–993.

6 K. Hasan, Y. Dilgin, S. C. Emek, M. Tavahodi, H.-E. Akerlund, P.-A. Albertsson and L. Gorton, *ChemElectroChem*, 2014, **1**, 131–139.
7 J. O. Calkins, Y. Umasankar, H. O'Neill and R. P. Ramasamy, *Energy Environ. Sci.*, 2013, **6**, 1891–1900.
8 A. Badura, T. Kothe, W. Schuhmann and M. Roegner, *Energy Environ. Sci.*, 2011, **4**, 3263–3274.
9 R. Tel-Vered and I. Willner, *ChemElectroChem*, 2014, **1**, 1778–1797.
10 T. Kothe, S. Poeller, F. Zhao, P. Fortgang, M. Roegner, W. Schuhmann and N. Plumere, *Chem. – Eur. J.*, 2014, **20**, 11029–11034.
11 F. Zhao, K. Sliozberg, M. Roegner, N. Plumere and W. Schuhmann, *J. Electrochem. Soc.*, 2014, **161**, H3035–H3041.
12 K. Hasan, H. B. Yildiz, E. Sperling, P. O. Conghaile, M. A. Packer, D. Leech, C. Hagerhall and L. Gorton, *Phys. Chem. Chem. Phys.*, 2014, **16**, 24676–24680.
13 P. Bombelli, R. W. Bradley, A. M. Scott, A. J. Philips, A. J. McCormick, S. M. Cruz, A. Anderson, K. Yunus, D. S. Bendall, P. J. Cameron, J. M. Davies, A. G. Smith, C. J. Howe and A. C. Fisher, *Energy Environ. Sci.*, 2011, **4**, 4690–4698.
14 P. Bombelli, T. Mueller, T. W. Herling, C. J. Howe and T. P. J. Knowles, *Adv. Energy Mater.*, 2015, **5**, 1401299.
15 R. W. Bradley, P. Bombelli, D. J. Lea-Smith and C. J. Howe, *Phys. Chem. Chem. Phys.*, 2013, **15**, 13611–13618.
16 J. M. Pisciotta, Y. Zou and I. V. Baskakov, *PLoS One*, 2010, **5**, e10821.
17 A. J. McCormick, P. Bombelli, A. M. Scott, A. J. Philips, A. G. Smith, A. C. Fisher and C. J. Howe, *Energy Environ. Sci.*, 2011, **4**, 4699–4709.
18 J. P. Giraldo, M. P. Landry, S. M. Faltermeier, T. P. McNicholas, N. M. Iverson, A. A. Boghossian, N. F. Reuel, A. J. Hilmer, F. Sen, J. A. Brew and M. S. Strano, *Nat. Mater.*, 2014, **13**, 400–408.
19 E. Stavrinidou, R. Gabrielsson, E. Gomez, X. Crispin, O. Nilsson, D. T. Simon and M. Berggren, *Sci. Adv.*, 2015, **1**, e1501136–e1501136.
20 M. Kasuno, M. Torimura, Y. Tsukatani, D. Murakami, S. Hanada, T. Matsushita and H. Tao, *J. Electroanal. Chem.*, 2009, **636**, 101–106.
21 Z. Chen, Y. Lyu, K. Wang, X. Dong, M. Deng, C. Bai, Y. Xu, W. Zhang and Z. Liu, *Int. J. Hydrogen Energy*, 2013, **38**, 13045–13049.
22 K. Hasan, K. V. R. Reddy, V. Essmann, K. Gorecki, P. O. Conghaile, W. Schuhmann, D. Leech, C. Hagerhall and L. Gorton, *Electroanalysis*, 2015, **27**, 118–127.
23 K. Hasan, E. Cevik, E. Sperling, M. A. Packer, D. Leech and L. Gorton, *Adv. Energy Mater.*, 2015, **5**, 1501100.
24 G. Longatte, H.-Y. Fu, O. Buriez, E. Labbe, F.-A. Wollman, C. Amatore, F. Rappaport, M. Guille-Collignon and F. Lemaitre, *Biophys. Chem.*, 2015, **205**, 1–8.
25 K. Maxwell and G. N. Johnson, *J. Exp. Bot.*, 2000, **51**, 659–668.
26 B. Genty, J. M. Briantais and N. R. Baker, *Biochim. Biophys. Acta*, 1989, **990**, 87–92.
27 K. A. Ahrling and S. Peterson, *Biochemistry*, 2003, **42**, 7655–7662.
28 B. A. Diner and V. Petrouleas, *Biochim. Biophys. Acta*, 1987, **893**, 138–148.
29 H. M. Gleiter, E. Haag, Y. Inoue and G. Renger, *Photosynth. Res.*, 1993, **35**, 41–53.
30 E. Haag, H. M. Gleiter and G. Renger, *Photosynth. Res.*, 1992, **31**, 113–126.
31 D. Joly and R. Carpentier, *J. Photochem. Photobiol., B*, 2007, **88**, 43–50.
32 D. Shevela and J. Messinger, *Biochim. Biophys. Acta, Bioenerg.*, 2012, **1817**, 1208–1212.
33 J. L. Zimmermann and A. W. Rutherford, *Biochim. Biophys. Acta*, 1986, **851**, 416–423.
34 S. Dudekula and M. Fragata, *J. Photochem. Photobiol., B.*, 2006, **85**, 177–183.
35 V. Petrouleas and B. A. Diner, *Biochim. Biophys. Acta*, 1987, **893**, 126–137.
36 K. Satoh, M. Ohhashi, Y. Kashino and H. Koike, *Plant Cell Physiol.*, 1995, **36**, 597–605.
37 Govindjee and J. J. Eatonrye, *Photosynth. Res.*, 1986, **10**, 365–379.
38 B. Rimbault, D. Esposito, D. Drapier, Y. Choquet, D. Stern and F. A. Wollman, *Mol. Gen. Genet.*, 2000, **264**, 486–491.
39 U. Schreiber, T. Endo, H. L. Mi and K. Asada, *Plant Cell Physiol.*, 1995, **36**, 873–882.
40 L. Houille-Vernes, F. Rappaport, F.-A. Wollman, J. Alric and X. Johnson, *Proc. Natl. Acad. Sci. U. S. A.*, 2011, **108**, 20820–20825.
41 X. Johnson, G. Vandystadt, S. Bujaldon, F.-A. Wollman, R. Dubois, P. Roussel, J. Alric and D. Beal, *Photosynth. Res.*, 2009, **102**, 85–93.